

**MASSACHUSETTS INSTITUTE OF TECHNOLOGY
HAYSTACK OBSERVATORY
WESTFORD, MASSACHUSETTS 01886**

August 21, 2018

Telephone: 617-715-5517

Fax: 617-715-0590

To: IVS VGOS Technology and Operations Groups

From: Brian Corey & Ed Himwich

Subject: Setting correlator clocks for VGOS CONT17 processing

1. Introduction

In June 2018 the VGOS CONT17 data were reprocessed at Haystack using a method of accounting for station delays that differs from the one used in the original January 2018 processing and in other VGOS processing to date. This memo describes the rationale behind adopting a new method and behind selecting the specific method used in June from among several options. This method can be used when processing VGOS data in any DiFX/HOPS-based geodetic VLBI correlator such as those at Haystack, Bonn, and WACO.

2. Clock models in general

The clock models specified in the \$CLOCK section of a VEX file have two functions in correlation:

- (a) Adjust the baseline *a priori* delay for the clock delays at the two stations in order to bring the residual singleband delay (SBD) close to zero (typically <100 ns).
- (b) Correct the time tag¹ associated with each data sample at a station for any error in the time tag applied at record time (i.e., in the VDIF epoch of the sample).

The latter correction is important when VLBI data are used to determine UT1-TAI (hereafter simply UT1), as a time-tag shift translates into a UT1 shift of the same magnitude and opposite sign [1]. See Appendix 1 for details on how \$CLOCK models affect observed delays.

The clock delay can be viewed crudely as made up of two parts:

- 1) the offset between UTC and the VDIF epoch assigned to the data samples (referred to in this memo as **VDIF-UTC offset**), and
- 2) the time difference between when a wavefront crosses the antenna intersection of axes and when its digitized sample is time-tagged in the backend (station instrumental delay, or simply **station delay**).

Up to now, standard VGOS practice has been to put only part 1 in the \$CLOCK section, with part 2 accounted for primarily by *sampler_delay_x/y* adjustments applied post-correlation by fourfit. These sampler delays are effectively added to the *a priori* delay in fourfit and so accomplish the first function above, but unlike \$CLOCK they do not affect the time tagging. (See Appendix 2 for confirmatory evidence.) In the original processing of the VGOS CONT17 sessions, the sampler delay differences between some station pairs were as large as 1.4 μ s. UT1 estimated from different baselines would therefore be inconsistent by up to 1.4 μ s.

¹ In this memo the term “time tag” refers either to the epoch associated with each data sample or to the mean epochs of the time-averaged correlated data (typically 1-second averages) passed through difx2mark4 to fourfit. It does *not* refer to the database parameter TIMETAG, which in HOPS is called the Fourfit Reference Time.

3. Clock models in S/X geodetic VLBI

The method used to create S/X clock models is an instructive starting point for VGOS.

In standard S/X correlation practice, all clock information goes into \$CLOCK; fourfit sampler delays are not used.

The initial estimates for the clock model offset and rate for a station are obtained by fitting a straight line to the dot2gps or fmout-gps time series in the Field System log. The sign conventions for dot2gps, fmout-gps, and \$CLOCK models are the same: a positive value means that dot, fmout, or the data sample time tag leads gps or UTC.

If these preliminary clock models are used to correlate a session, residual SBDs will typically be between a few hundred ns and a few μ s, depending on baseline. These large biases reflect mainly the missing “part 2” instrumental delays of section 2. On a given baseline the *rms* scan-to-scan scatter in X-band residual SBD for high-SNR scans or in the more precise X-band residual multiband delay (MBD) for all scans is generally <10 ns. This fact indicates that, aside from the clock model, the *a priori* model based on station and source positions, EOP, and a tropospheric delay model is good to <10 ns. (The scatter can be larger at S-band due to unmodeled ionospheric delay contributions.) By adjusting the preliminary dot2gps-based clock model for each station by a station-specific amount, the X-band residual SBD on each baseline can be brought much closer to zero, typically within <10 ns.² This adjustment is called the **peculiar offset**. The resulting clock models should be accurate at X-band to <10 ns, aside from an overall additive constant – a **universal clock adjustment (UCA)**, if you will – that can be applied to all models without affecting the baseline *a priori* delay.

With clock models consistent to a few tens of ns, UT1 estimated from different baselines should be consistent at the same level. If the UCA applied to all models is changed, however, UT1 will change by that amount. In order to avoid jumps in UT1 time series caused by such a change, IVS correlators use a standard set of peculiar offsets that ultimately can be traced back to setting the peculiar offset for KOKEE20M to zero in the 1990s. The KOKEE20M instrumental delay was of course not truly zero, so the S/X UT1 time series is biased compared with an “absolute” time series wherein UT1 is the Earth rotation angle determined by a fictitious zenith-pointing telescope.

4. Goals

The main aim in revising the VGOS processing procedure is to move as much of the station delay as possible into \$CLOCK so that the data time tags, and hence correlated data time tags and UT1 estimates, are consistent among stations and baselines within a session. Maintaining consistency from session to session is also important, but we do not address that topic here.

The level of consistency should be small compared with the formal UT1 error in a daily geodetic session. For the CONT17 VGOS series, the formal error was ~ 800 ns. We therefore set as a goal that data time-tagging be consistent among all stations to <100 ns.

There is also the question of the value of the UCA to be applied to all peculiar offsets, i.e., how do we want to bias the VGOS UT1 time series. There are at least three options:

² Residual SBD can differ between S- and X-band for a given station by as much as ~ 100 ns due to differences in instrumental delays. Because X-band data are much more heavily weighted than S-band when constructing the ionosphere-free delay, standard practice is to adjust the clock model to minimize the X-band residual SBD bias.

- (a) Set the peculiar offset arbitrarily (to zero, say) for one site. The offsets for the other sites will follow by requiring residual SBD = 0. This is the S/X example.
- (b) Set the UCA so that the VGOS UT1 time series is unbiased relative to the S/X.
- (c) Set the UCA to give an “absolutely” correct time series.

Option (a) is the easiest. Geodetic sessions already observed (e.g., the KT series with KOKEE20M and KOKEE12M or mixed-mode R1 sessions) may provide the information needed to enable option (b), but they have not yet been analyzed toward that end. Option (c) requires careful measurements of instrumental delays at a VGOS site (and preferably at multiple sites to check consistency); such measurements have not yet been carried out to our knowledge. Note that, because a change in UCA shifts UT1 by the same amount, a future decision to change from one of the above options to another can be applied retroactively to existing UT1 time series simply by applying an additive constant.

5. Options for setting VGOS clocks

Putting aside temporarily the question of what value to assign to the UCA, we list three options for how the \$CLOCK models and fourfit sampler delays could be set so as to incorporate most, if not all, the station delay into \$CLOCK. We assume the present incarnations of DiFX and HOPS, without any code modification or augmentation. In this section we consider only stations with instrumental delays that vary from band to band by $\lesssim 100$ ns. We defer to the next section treating the one form of large band delay differences encountered on a regular basis to date, *viz.*, large differences between bands A and B-D.

- (a) Leave the fourfit *samplers* command undefined so that the SBD is not adjusted by the ‘PC delays’³ listed on a fourfit plot. Set the peculiar offset for one station to zero, then set the peculiar offsets for the others by requiring residual SBD = 0. This method is akin to the S/X and gives peculiar offsets closest to their true values, to within limits imposed by the band-to-band delay variation for each station. Because *samplers* is undefined, cross-spectral phases will not be corrected for instrumental phase variations over frequency or time, and multitone phases will be used only to calculate the mid-channel phase cal phases to be applied for MBD estimation. A drawback is that dispensing with the cross-spectral phase corrections will decrease SNR and precision. Far more serious is the fact that, by not correcting the SBD within each band for the mean PC (i.e., instrumental) delay at each station, the residual SBD will vary from band to band by tens of ns or more at some sites (and by ~ 325 ns between bands A and B-D at GGAO12M). When the peak-to-peak SBD variation across bands is not small compared with the inverse channel bandwidth (currently $1/32 \mu\text{s}$), significant coherence loss will occur when fringe-fitting across all bands, as is standard for VGOS.
- (b) Same as (a) except that, after determining the peculiar offsets, define *samplers* and set *sampler_delay* for each band/polarization to the median⁴ observed PC delay in the default range between -100 and +100 ns. Residual SBDs on a given baseline will now be consistent across bands, and SNR will be improved over (a). Residual SBDs will however be nonzero by as much as 200 ns due to their now being affected by the PC delays, and they will differ from baseline to baseline. This fact will greatly complicate monitoring changes in the clock

³ ‘PC delay’ represents the difference in signal delay between the paths (a) from maser to phase cal generator in the receiver to sampler and (b) from maser to sampler clock circuit. The PC delay shown on a fourfit fringe plot for each channel is the phase cal delay calculated from the unmasked phase cal tones in the channel, subject to the requirement that its value lies within a 200-ns-wide range whose midpoint is specified by the *sampler_delay_x/y* parameter for the band and polarization of the channel. If *sampler_delay* is not specified, PC delay defaults to the value between -100 and +100 ns. Iff the fourfit *samplers* command is defined (by which is meant that one or more sets of channels are defined that share a common physical sampler and so should have similar delays), the mean PC delay over the sampler pool is used to correct the SBD.

⁴ Or mean delay – the precise value is not critical since *sampler_delay* defines only the range within which PC delay is to lie, not its actual value.

delays from session to session, as one cannot rely on a nonzero residual SBD as indicating a clock change as in the current method.

- (c) Same as (b) but define *samplers* and *sampler_delay* values from the start. Residual SBDs will be near zero across all bands and baselines, but the clock models will be in error by the amount of the PC delay, *i.e.*, by up to 100 ns (half a phase cal ambiguity).

A fourth option differs from (c) only in the UCA value:

- (d) The January 2018 CONT17 correlation was set up in a manner similar to (c) except that the *sampler_delay* values included multiple 200-ns ambiguities that brought them as close as possible to the values for the receiver-to-backend station delays⁵ estimated by Arthur Niell. Consequently the peculiar offsets were small (<100 ns). Achieving the goal stated at the beginning of section 4 entails simply, for each site, moving the integer phase cal ambiguities in the January 2018 sampler delays that are common across bands and polarizations out of the sampler delays (so that the new sampler delays are in the range ± 100 ns) and into the clock model. For example, if the old sampler delay is 1180 ns, subtract 1200 ns so that its new value is -20 ns, and add 1200 ns to the clock offset. The residual SBDs should be the same as before the change, with absolute values <10 ns typically. As in (c), the clocks will be wrong by up to 100 ns.

Option (d) was chosen for the June 2018 CONT17 reprocessing because it lacks the drawbacks of (a) and (b) and because it comes as close to providing absolute UT1 as we can at present, unlike (c). To the extent the January station delay estimates are accurate (and ignoring the relatively small difference between epochs of wavefront reception in the feed and of wavefront passage by the intersection of axes), UT1 estimates based on data processed with option (d) should be absolute to <100 ns.

When the new method was first tested, an unanticipated bonus (subsequently explained by Roger Cappallo) was an SNR increase by up to ~40%, with the increase roughly proportional to the absolute magnitude of the change in reference-remote sampler delay difference.

6. Dealing with the band A delay offset

At GGAO12M and KOKEE12M, the instrumental delay in band A differs from that in bands B-D by ~300 ns due to using coax for the band A downlink and fiber for B-D. As described in Appendix 3, time-tag errors induced by the difference in band delays can be kept under ~30 ns (or equivalently the corresponding MBD errors can be kept under 30 ns times delay rate) by setting the peculiar offset as close as possible to midway between the band A and band B-D delays.

7. Detailed procedure

Here we describe in detail how the \$CLOCK model and fourfit control file used in the January 2018 CONT17 processing were modified for each station in the June reprocessing, in accordance with the recommended option (d) of section 5 and with section 6. The initial fourfit *sampler_delay* values are those determined by Arthur Niell and used in the January 2018 processing. In all cases, *sampler_delay* was identical for X and Y polarizations.

- 1) Let SD_A be the *sampler_delay* value for band A, and SD_{BCD} be the mean of the *sampler_delay* values for bands B-D.

⁵ Because sampler (or PC) delay and station delay refer to different, albeit overlapping, signal paths, in general the sampler delay cannot be made to match the station delay by adding 200-ns ambiguities. For the optimum number of ambiguities, the two delays will differ by up to 100 ns.

- 2) Set $SD_{\text{all}} = (SD_A + SD_{\text{BCD}}) / 2$.
- 3) Set $SD_{\text{mod}} = SD_{\text{all}} \text{ modulo } 200 \text{ ns}$, with $-100 \text{ ns} \leq SD_{\text{mod}} \leq 100 \text{ ns}$. SD_{mod} is the *sampler_delay* with phase cal ambiguities removed.
- 4) Set $SD_{\text{amb}} = SD_{\text{all}} - SD_{\text{mod}}$. SD_{amb} will be an integer multiple of 200 ns.
- 5) Add SD_{amb} to the \$CLOCK offset.
- 6) Subtract SD_{amb} from all 8 *sampler_delay* values (4 bands and 2 pols) in the fourfit control file.

When this procedure was applied to the six stations in CONT17, the new SD_{all} values ranged from -62 ns to 20 ns. These values also correspond to the relative \$CLOCK offset errors between stations, and they meet the target of consistent time-tagging among stations to <100 ns.

References

- [1] Himwich, W.E., *et al.*, "Impact of station clocks on UT1-TAI estimates," Proceedings 23rd EVGA Meeting, http://www.evga.org/files/2017EVGA_proc_Gothenburg.pdf#section*.324, 2017.
- [2] Corey, B., "Conversion from Mark IV to Mark III delays and rates," MIT Haystack Observatory memorandum, 2000 January 27.
- [3] Corey, B., and Titus, M., "Multiband delay differences between Mk4 hardware and DiFX software correlations," MIT Haystack Observatory memorandum, 2012 September 18.

Appendix 1. Effect of changing \$CLOCK model on fourfit delay

The *a priori* delay on a baseline can be viewed as the sum of two components: the “geometric” delay from CALC (which includes tropospheric delay) and the clock delay difference between the stations. Let A and B be the labels for the reference and remote stations. If the \$CLOCK offsets for the two stations are changed by δ_A and δ_B , the *a priori* baseline clock delay changes by $\delta_B - \delta_A$ (this is effect (a) in section 2 of the memo). In contrast, the time-tag shift that accompanies a change in clock delay (effect (b) in section 2) does not affect the *a priori* delay. Of the delays reported by fourfit, only the total and residual delays, but not the *a priori* delay, can be affected by a time-tag shift.

The Mk3 correlator used a reference-station time base in the sense that the Fourfit Reference Time (FRT) is the reception epoch of the wavefront at the reference station, and the data samples and correlated data are time-tagged based on the reference station time tags. To see what happens when the clock model is changed, let the total delay be expressed as $\tau_{\text{tot}}(t_0) \equiv \tau_{\text{geo}}(t_0) + \text{clock}_B(t_0) - \text{clock}_A(t_0) + \tau_{\text{res}}(t_0)$, where the first three terms make up the *a priori* delay, the fourth is the residual delay, and t_0 is the FRT. If the clock offsets are now shifted by δ_A and δ_B , the time tags at the reference station get shifted by $-\delta_A$. As a result, the total delay at the FRT will change from $\tau_{\text{tot}}(t_0)$ to $\tau_{\text{tot}}(t_0 + \delta_A)$ due to the time-tag shift, the *a priori* delay will change by $\delta_B - \delta_A$, and the residual delay will change by $\tau_{\text{tot}}(t_0 + \delta_A) - \tau_{\text{tot}}(t_0) - \delta_B + \delta_A$. To first order in the delay time derivatives, the change $\tau_{\text{tot}}(t_0 + \delta_A) - \tau_{\text{tot}}(t_0)$ in total delay is $\dot{\tau}_{\text{tot}}(t_0) \delta_A$. It is this dependence on delay rate that leads to a shift in solved-for UT1 when clock models are changed.

Unlike the Mk3 correlator, a DiFX/HOPS correlator uses geocentric delay models and a geocentric time frame in the sense that the FRT is the reception epoch of the wavefront at the geocenter. Because most (all?) geodetic VLBI analysis software packages assume a Mk3-style reference-station time base, the delays and rates from a DiFX correlator are converted in HOPS to a Mk3 frame before being entered in a geodetic database. This conversion affects the geometric portion of the *a priori* delay (see, e.g., [2]) but not the clock delay. Because the geocentric and Mk3-converted residual delays are expected to differ by $< \sim 0.2$ ps for residual rates < 10 ps/s [2], the Mk3-converted residual delay is set equal to the geocentric residual delay in HOPS. Hence in HOPS there is no distinction between Mk3 and geocentric residual delay.

The time-tag delay shift in a DiFX/HOPS correlator can be analyzed in a similar manner to the Mk3 treatment above. The *a priori* delay is the delay difference between the two geocenter-to-station delays: $\tau_{\text{ap}}(t_0) \equiv \tau_B(t_0) - \tau_A(t_0)$, where each τ_X is the sum of geometric and clock terms; the total delay can be expressed in like manner. If the clock offsets are now shifted by δ_A and δ_B , the total delay will change by $[\tau_B(t_0 + \delta_B) - \tau_B(t_0)] - [\tau_A(t_0 + \delta_A) - \tau_A(t_0)] = \dot{\tau}_B(t_0) \delta_B - \dot{\tau}_A(t_0) \delta_A$, to first order in delay time derivatives. In the special case $\delta_A = \delta_B \equiv \delta$, the change in total delay is simply $\dot{\tau}_{\text{tot}}(t_0) \delta$.

Appendix 2. Tests of effect of universal \$CLOCK or sampler delay shift on fourfit delay and rate

As described in [1], tests of the effect of shifting all \$CLOCK models by the same amount have been conducted in which an entire Intensive session was correlated twice, once with clocks shifted and once unshifted. The difference in UT1 values estimated from the correlated data matched the clock shift in magnitude and sign, as expected.

A finer-grained test is to examine the effect on the fourfit total delay and rate for individual scans.

In fourfit, the total delay at an arbitrary epoch during a scan is modeled as the sum of the *a priori* delay at epoch FRT and the residual delay model evaluated at the arbitrary epoch, where the residual model consists of a constant (i.e., the delay at the FRT) plus a rate term. If the \$CLOCK models for all stations are shifted by the same amount δ , the total delay will be unchanged if the FRT is shifted by $-\delta$. On the other hand, if FRT is held fixed, the total delay will be the original delay at epoch FRT + δ .

The last two statements require minor qualification in two regards. First, the statements hold provided δ is small enough and/or the scan length short enough that the residual phase vs. time and frequency during the scan is well described by fourfit's linear functions of time and frequency. If δ is several seconds, say, mismatch between the *a priori* and actual fringe acceleration may be large enough to cause significant quadratic curvature in the residual phase time series. As a result, the delay and rate fit to the residual time series will be in error. Second, imperfections in the digital correlation process lead to differences between expected and observed delay changes, typically at the level of a small fraction of the formal error. Correlator repeatability tests provide evidence of this effect. For example, Corey and Titus [3] found that, for small clock shifts of order 0.1 μ s and 1 ps/s, the *rms* change in total MBD for a DiFX correlator was ~ 0.15 times the undifferenced MBD standard error. Any change attributable to the time-tag shift would have been far smaller.

Because the FRT can be changed only in steps of integer seconds in HOPS, tests of the effect of a universal \$CLOCK shift are usually done with the FRT held fixed. In this appendix we provide the results of a few such tests after first outlining the "theory".

Calculated change in total delay and rate

Express the total delay time dependence as a fourth-order Taylor series about the FRT t_0 :

$$\tau(t) = d_0 + d_1 (t-t_0) + d_2 (t-t_0)^2 + d_3 (t-t_0)^3 + d_4 (t-t_0)^4$$

Let the input data span a time interval $2T$ centered on t_0 .

The change in delay and rate caused by adding δ to all \$CLOCK values can then be calculated to be

$$\Delta\tau = d_1 \delta + d_2 \delta^2 + d_3 \delta^3 + d_4 \delta^4 + (d_3 \delta + 2 d_4 \delta^2) T^2$$

$$\Delta\dot{\tau} = 2 d_2 \delta + 3 d_3 \delta^2 + 4 d_4 \delta^3 + 12 d_4 \delta T^2 / 5$$

Note that, exclusive of the trailing term proportional to T^2 , the expected change in delay or rate is simply the Taylor series expression for delay or rate evaluated at $t = t_0 + \delta$ minus the delay or rate at $t = t_0$.

"Observed" change in total delay and rate

Two scans, one from RD1702 and one from RD1508, were each correlated thrice, once with nominal \$CLOCK models and then twice more, each time with a common shift applied to the clock offset for all models. The representative results in Table 1 were obtained from fringing the 8 USB X-band channels.

“O” is the observed change in total delay or rate, “C” the calculated change from the equations above, and σ the standard error of the associated undifferenced parameter.

Table 1. Effect on total MBD and delay rate of applying a common clock shift to all stations.

<i>baseline</i>	δ	multiband delay (ps)				delay rate (fs/s)			
		$\Delta\tau_{obs}$	$\Delta\tau_{O-C}$	<i>MBD</i> σ	$(O-C)/\sigma$	$\Delta\dot{\tau}_{obs}$	$\Delta\dot{\tau}_{O-C}$	<i>rate</i> σ	$(O-C)/\sigma$
Ny-Wz	8 μ s	-6.3	-1.3	8.2	-0.16	0.2	0.3	22.0	0.12
Hh-Kb	100 μ s	218.3	0.4	3.7	0.11	-1.8	-2.1	7.6	-0.16
Hh-Ny	100 μ s	90.2	-0.7	8.6	-0.08	-7.1	-2.6	17.0	-0.15
Kb-Ny	100 μ s	-128.3	-0.2	3.2	-0.06	-5.8	-1.0	6.7	-0.15
Kb-Ny	1100 μ s	-1408.2	0.7	3.2	0.22	-55.0	-1.7	6.7	-0.25
Ny-Wz ⁶	1 second	-615805.7	3.1	8.6	0.36	-6276.5	-51.7	23.6	-2.19

RD1508: Scan 281-0344 with stations NYALES20 (Ny) and WETTZELL (Wz)

RD1702: Scan 025-0344 with stations HARTRAO (Hh), KASHIM43 (Kb), and NYALES20 (Ny)

Table 1 demonstrates good agreement between observed and expected delay and rate shifts. In particular, observed and calculated delays agree to $<0.4 \sigma$ (column 6) and, in the Ny-Wz 1-second case in the last row, to 1 part in 2×10^5 (ratio between columns 3 and 4). Rates are also well predicted except for the Ny-Wz 1-second case.

Effect of universal shift in fourfit sampler delays

In contrast with \$CLOCK, universal *sampler_delay* shifts do not affect fourfit delays, as shown by tests carried out on WESTFORD-WETT13S data for VT7142 scan 143-1738. Fringing was done for polarization Ixy with a control file that differed from the production file in two regards: only the eight band B channels were included, and no ionospheric delay fit was done. When the sampler delays for both sites were changed by 200 ns, SBD and MBD were unchanged to < 0.01 ps. If sampler delays affected time tagging in the same manner as \$CLOCK models do, the fourfit delays should have changed by the product of 200 ns and the total delay rate, which in this case is 0.27 ps. The fact that the fourfit delays did not change implies that fourfit does not adjust time tags for sampler delay.

⁶ For the Ny-Wz $\delta=1$ s case in the last row, the combination of a large value for δ and a long scan (440s) leads to a simple linear model in time being a poor model for the residual phase time series. The scan was therefore fringed in eleven contiguous 40-s-long segments, with the FRT set to the midpoint of each segment. The table values for observed $\Delta\tau$ and $\Delta\dot{\tau}$ (columns 3 and 7) are those of the middle segment, and the corresponding O-C values (columns 4 and 8) are the means of the eleven individual O-C values.

Appendix 3. Setting \$CLOCK when band A delay differs from band B-D delay

In this appendix we treat how to set the \$CLOCK model for a station where the instrumental delay for band A differs from that for bands B-D by > 100 ns.

Start by considering an ideal case where for each station all four bands have the same station delay and same VDIF-UTC offset, and the fringe phases for all 32 channels are zero. (Real-world fringe phases can be made zero by applying pc_phases_x/y in fourfit.) Now let one or more bands at a site have an additional station delay δ relative to the other bands. If no changes are made in \$CLOCK, there will be two changes to the pre-fourfit fringe phases⁷ in the bands with the added delay:

- 1) they will shift by $v_{RF} \delta$ due to the direct effect of delay on phase, and
- 2) they will shift by $v_{RF} \dot{\tau} \delta$ due to the time-tag effect of Appendix 1, where $\dot{\tau}$ is the geocenter-to-station delay rate.

In fourfit the phase cal correction eliminates the first type of shift from the residual fringe phases, but the time-tag shift remains. Note that the latter cannot be removed with fixed pc_phases_x/y values for an entire session because the phase shift depends on $\dot{\tau}$, which varies from scan to scan.

In fourfit a function of the form $\varphi_0 + \text{MBD} (v_{RF} - v_0) + K_{\text{ion}} / v_{RF}$ is fit to fringe phase vs. RF frequency⁸, where the last term represents the ionospheric, or ‘dTEC’, delay. When this function is fit to fringe phases of the sort described in the preceding paragraph, the MBD and K_{ion} values will in general be nonzero. Figure 1 shows the MBD and dTEC functions for the 15 possible combinations of bands with a delay offset, and Table 2 lists the MBD and K_{ion} values. RF frequencies are those for CONT17, and fringe amplitudes are assumed to be flat over frequency. The four identifying integers for each combination refer to bands A-D, with a ‘1’ signifying an offset δ is present and a ‘0’ signifying no offset.

Of relevance to the issue of stations with a large instrumental delay offset between band A and bands B-D are the two cases ‘1 0 0 0’ (top left panel in Figure 1) and ‘0 1 1 1’ (bottom middle panel). Their MBD values are both $0.50 \dot{\tau} \delta$, and their K_{ion} values have the same magnitude and opposite sign.⁹

With these two results in hand, one can calculate a clock peculiar offset δ_0 for which the MBD is zero when fitting to the band-dependent time-tag fringe phases. Let δ_A be the station delay for band A, and let δ_{BCD} be the delay for B-D. From the results cited in the preceding paragraph, the net MBD relative to δ_0 is $0.5 \dot{\tau} (\delta_A - \delta_0) + 0.5 \dot{\tau} (\delta_{\text{BCD}} - \delta_0)$. Setting this expression to zero yields $\delta_0 = 0.5 (\delta_A + \delta_{\text{BCD}})$. The effect of band-dependent station delays on MBD can thus be eliminated by setting the peculiar offset to midway between the band A and bands B-D station delays¹⁰.

⁷ The sign of the phase shift will be positive or negative depending on whether the station is reference or remote, but that fact will prove to be irrelevant.

⁸ The delay rate and SBD observables that fourfit also estimates are ignored here.

⁹ Because least-squares is a linear process, the MBD and K_{ion} values for two complementary combinations like ‘1 0 0 0’ and ‘0 1 1 1’ must sum to the MBD and K_{ion} values for ‘1 1 1 1’. The latter values are $\dot{\tau} \delta$ and zero, respectively – see bottom right panel in Figure 1 and last line in Table 2. That ‘1 0 0 0’ and ‘0 1 1 1’ have K_{ion} values of opposite sign is therefore to be expected. That they have the same MBD values appears to be purely coincidental, as that is not true for other frequency sequences or when fringe amplitudes are not assumed flat.

¹⁰ By a similar argument, in the general case of different station delays in all 4 bands, the peculiar offset δ_0 that eliminates this effect is $0.500 \delta_A - 1.441 \delta_B - 1.449 \delta_C + 3.390 \delta_D$ when fringe amplitudes are flat. The four coefficients are the MBD values in the first four lines of Table 1.

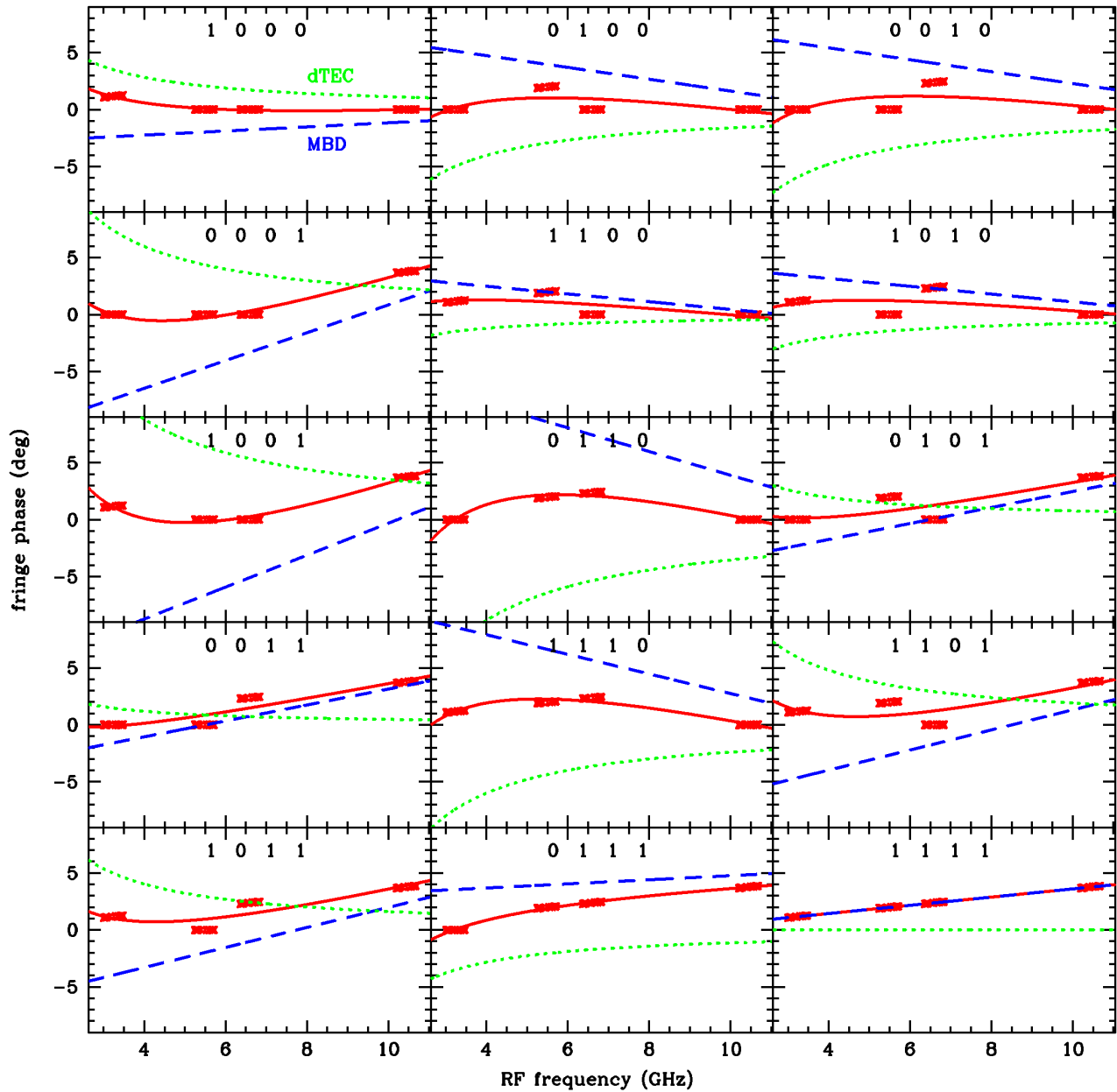


Figure 1. MBD + dTEC model fits to channel fringe phase vs. frequency for 15 combinations of bands for which fringe phase is offset from zero by $\nu_{RF} \tau \delta$. The four integers in each panel refer to bands A-D, respectively, with '0' meaning no offset and '1' meaning an offset is present. Channel frequencies are those of CONT17, and fringe amplitudes are the same in all channels. Red 'X' = channel fringe phase, dashed blue line = best-fit MBD + phase offset, dotted green line = best-fit ionospheric 'dTEC' model, red solid line = MBD + dTEC models. Units for fringe phase ordinate are degrees when $\tau \delta = 1$ ps.

Table 2. Parameter values from model fits shown in Figure 1.

Fringe phase offset present? (0=no, 1=yes)				MBD (units of $\tau \delta$)	K_{ion} (units of $\tau \delta \text{ deg GHz}^2$)
<i>band A</i>	<i>band B</i>	<i>band C</i>	<i>band D</i>		
1	0	0	0	0.500	11 330
0	1	0	0	-1.441	-16 100
0	0	1	0	-1.449	-19 190
0	0	0	1	3.390	23 960
1	1	0	0	-0.941	-4 771
1	0	1	0	-0.949	-7 864
1	0	0	1	3.890	35 290
0	1	1	0	-2.890	-35 290
0	1	0	1	1.949	7 864
0	0	1	1	1.941	4 772
1	1	1	0	-2.390	-23 960
1	1	0	1	2.449	19 190
1	0	1	1	2.441	16 100
0	1	1	1	0.500	-11 330
1	1	1	1	1.000	0

Depending on the clock-setting procedure (see section 5), it may not be possible to set the peculiar offset precisely to the midway station delay. To apply procedure (c) or (d) to the situation at hand, the only modification needed to the description in section 5 is that now it is the mean of the band A and bands B-D *sampler_delay* values that is to be set between -100 and +100 ns. The peculiar offset will differ from the midway station delay by that mean value (or, strictly speaking, by the mean of the band A and bands B-D PC delays), and the time-tagging will be in error by the same amount.

As a test of the robustness of this method *vis-à-vis* fringe amplitude differences among bands, the best-fit ‘1 0 0 0’ and ‘0 1 1 1’ MBD values were determined with weighted least-squares for the 15 independent cases where fringe amplitudes were the same for all channels in a band but could differ from band to band, with a value of either 1 or 2. The best-fit MBD values were all between $0.4 \tau \delta$ and $0.6 \tau \delta$, not far from the $0.5 \tau \delta$ found for flat amplitudes. The maximum difference of $0.1 \tau \delta$ from the flat-amplitude value leads to a maximum error in the net MBD of $0.60 \tau (\delta_A - \delta_{BCD}) / 2 - 0.40 \tau (\delta_A - \delta_{BCD}) / 2 = 0.1 \tau (\delta_A - \delta_{BCD})$. For $|\delta_A - \delta_{BCD}| = 300 \text{ ns}$, the maximum error from non-flat amplitudes is equivalent to the time-tag error caused by a 30-ns error in \$CLOCK.

For frequency sequences other than CONT17 (e.g., that proposed by Bill Petrachenko in a 2018 April 1 email), the parameter values will differ from those in Table 2, and the ideal station delay to use in \$CLOCK will accordingly differ from the mean A + BCD delay found for CONT17. In some test cases it was found that the MBD parameter was much more sensitive to band dependence in the fringe amplitudes than for the CONT17 sequence. In such cases the maximum error from non-flat amplitudes may be unacceptably large.